LOW FREQUENCY DIELECTRIC DISPERSION OF CLAY-WATER-ELECTROLYTE SYSTEMS

KANDIAH ARULANANDAN

Department of Civil Engineering,
University of California, Davis, California

and

JAMES K. MITCHELL

Department of Civil Engineering,
University of California, Berkeley, California

Abstract—The dielectric properties of saturated kaolinite clay-water-electrolyte systems were determined over the frequency range of $30-10^5$ c/s. Very large dielectric constants are observed at low frequencies. Since the experimental data approach constant values at each end of this frequency spectrum, they can be described by a fairly well defined spectrum of relaxation times. The particle size and orientation, the type and amount of electrolyte, and temperature affect the low frequency dielectric increment and the average relaxtion time. Several physical processes, such as relaxtion due to dipolar rotational polarization, interfacial polarization, free space charge and bound ion polarization, are examined in an attempt to explain the observed data. It is concluded that there exists at present no theory to explain all the data, but the bound ion polarization mechanism appears to explain some of the results.

INTRODUCTION

THE electrical properties of clay-water-electrolyte systems are potentially useful for the study of clay structure, Arulanandan (1966), Mitchell and Arulanandan (1967), for electrical prospecting in geophysical work, and for study of ion transport properties, Madden and Marshall (1958, 1959). Considerable information on the electrical properties of solid, liquid or solid-liquid mixtures in an alternating current field has been obtained (see references). It has been observed experimentally that the dielectric constant, ϵ', decreases and the conductivity, σ, increases with increase in frequency in a variety of materials (Figs. 1, 2). There have been suggestions that the variation of conductivity and dielectric constant with frequency (generally described as the dispersion characteristics) may result from:

1. Polarization due to molecular rotation either in polar liquids or in solid polar liquid mixtures, Debye (1929).
2. Polarization due to accumulation of charges at interfaces of different media in colloidal suspension of low volume concentrations, Maxwell-Wagner (1914), and in high volume concentration, Pauley and Schwan (1959).
3. Polarization due to ion atmosphere displacement, O'konski (1960), Schwarz (1962), Mandel (1963).

4. Polarization due to diffusion coupling between ion flows, Madden and Marshall (1959).

In the present work, the dielectric properties of kaolinite-clay-water-electrolyte systems are reported for a range of frequencies, and the results are discussed in terms of the existing theories of mechanisms of conduction.

EXPERIMENTAL

Instrumentation

Impedances were measured with a "Comparator," type 1605 AM (General Radio Corporation). This instrument is essentially a wheatstone bridge with a sensitive visual null indicator. Series of measurements of the impedances of clay-water-electrolyte systems were carried out within the frequency range 100–100,000 c/s using the comparator. Since the comparator only enables determination of capacitance and resistance at frequencies of 100 c/s, 1000 c/s, 10,000 c/s and 100,000 c/s, a special low frequency bridge was developed for measurements at 30 and 300 c/s. Figure 3 shows schematically the details of this low frequency bridge.

At each frequency the bridge was balanced with a standard capacitance and resistance. The value of standard resistance chosen was nearly equal to
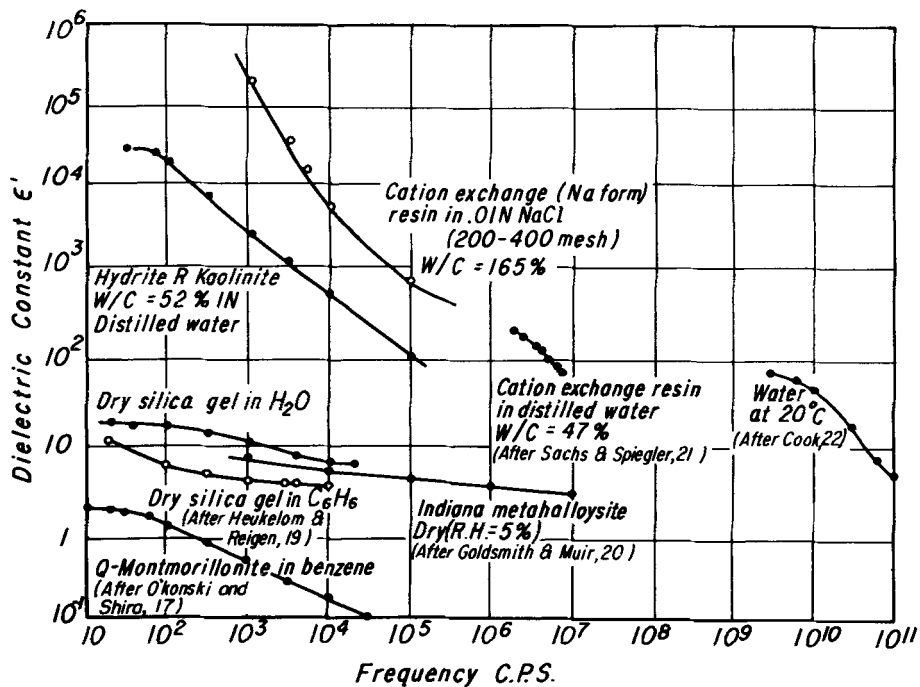
Fig. 1. Dielectric behaviour of clay-water and ion exchange resin systems.

that of the soil sample. Standard capacitances of 0·01 μf and 150 $\mu\mu f$ were used at 100 c/s and at 1000, 10,000, 100,000 c/s respectively. The standard resistance was then removed and the cell with the soil sample connected in parallel with the standard capacitance and the bridge balanced again. The values of capacitance and resistance of an equivalent parallel circuit of these two components were read directly on the instrument. The instrument readings gave the resistance of the sample, the capacitance of the sample, the capacitance due to electrode polarization and the standard capacitance. The standard capacitance was substracted from the instrument reading to obtain the sample capacitance and the effects due to electrode polarization.

The design of the sample cell and the connections to the bridge terminals enabled measurements of soil columns of different length and thus elimination by computation of the appreciable influence of electrode polarization, especially at the very low frequencies. The cylindrical sample was held between two flat circular platinum electrodes which were platinum black coated. The distance between these electrodes could be changed and thus samples of different lengths could be tested in a manner similar to that used by Gillespie and Cole (1956) for measurements of dielectric constant of

sulfuric acid and by Mandel for electrolyte and polyelectrolyte solutions (1963).

Analysis of data

The measured impedances were interpreted in terms of circuits of the type shown in Fig. 4 (a) and (c). These networks consist simply of two impedances in series. One of these series impedances, Z_{tr}, represents the electrode polarization impedance, the other composed of a resistance and a capacitance in parallel (R_s, C_s and R_s/l, $C_s l$ in Fig. 5 (a) and (c) for samples whose lengths are in the ratio l respectively), represents the sample.

Equating the expressions for the impedances of circuits (a) and (c) obtained from elementary network analysis, LePage (1952), to those of (b) and (d), respectively, one obtains two equations of complex variables from which the electrode polarization impedance, Z_{tr}, can be eliminated. The real and imaginary parts of the resulting single equation then lead to Eqs. (1) and (2) for the true resistance (ohms) and capacitance ($\mu\mu f$) of the sample, respectively, at frequency, f (sec^{-1}).

Equations (1) and (2) contain R_p, C_p, R'_p and C'_p which are read directly from the comparator and the low frequency bridge at the frequency, ω. By performing these measurements at different frequencies, the source data were obtained.

$$R_s = \frac{\left[\dfrac{R_p{}^2 C_p}{1+\omega^2 R_p{}^2 C_p{}^2} - \dfrac{R_p'{}^2 C_p'}{1+\omega^2 R_p'{}^2 C_p'{}^2}\right]^2 (1+R_p{}^2\omega^2 C_p{}^2)(1+R_p'{}^2\omega^2 C_p'{}^2)\, l\omega^2}{[R_p(1+R_p'{}^2\omega^2 C_p'{}^2) - R_p'(1+R_p{}^2\omega^2 C_p{}^2)]\,(l-1)}$$

$$+ \frac{[R_p(1+R_p'{}^2\omega^2 C_p'{}^2) - R_p'(1+R_p{}^2\omega^2 C_p{}^2)]\, l}{(1+R_p{}^2\omega^2 C_p{}^2)(1+R_p'{}^2\omega^2 C_p'{}^2)\,(l-1)} \qquad (1)$$

$$C_s = \left[\frac{(1+R_P\,\omega^2 C_P{}^2)(1+R_{P'}{}^2 C_{P'}{}^2\omega^2)(l-1)}{R_s\omega^2 R_P(1+R_{P'}{}^2 C_{P'}{}^2\omega^2) - R_P(1+R_P{}^2\omega^2 C_P{}^2)\,l} - \frac{1}{R_s{}^2\omega^2}\right]^{1/2} \qquad (2)$$

Conductivity (σ) mhos/cm; thd dielectric constant (ϵ'); and dielectric loss, $\epsilon'' = (\sigma - \sigma_0/\omega\epsilon_r)$, where σ_0 is the D. C. conductivity; $\omega = 2\pi f$; and $\epsilon_r = 8{\cdot}85 \times 10^{-14}$ F/cm, the dielectric constant in vacuum, were obtained by use of the expressions

$$\sigma = \frac{d}{R_s A} \qquad (3)$$

$$\epsilon'\epsilon_r = \frac{C_s d}{A} \qquad (4)$$

Where d is the length and A the cross-section area of the sample.

These values of σ, ϵ' and ϵ'' depend only on the structure and composition of the material, provided the values of R_s and C_s are independent of voltage. The measurements of R_s and C_s were made at such low intensities of applied voltage that Ohm's law was fulfilled thus insuring the required voltage independence. In all measurements a current density less than 10^{-3} amps/cm² was used and found to be satisfactory.
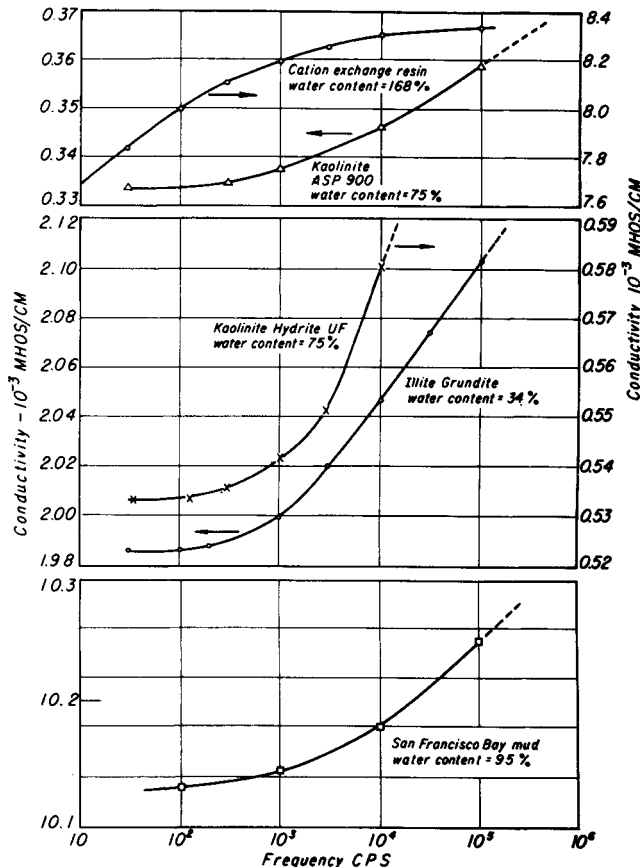

Fig. 2. Conductivity dispersion of clays and cation exchange resin.

R₁-R₂ *Matched resistors to complete bridge*
R₃   *Resistance decade box*
C₁   *Capacitance*
T₁   *Transformer to isolate bridge network from oscillator ground.
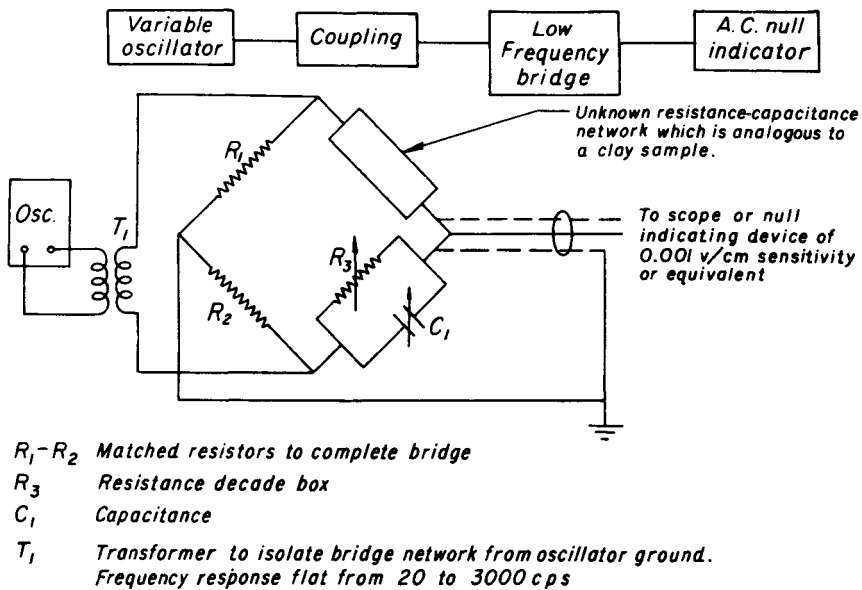   Frequency response flat from 20 to 3000 cps*

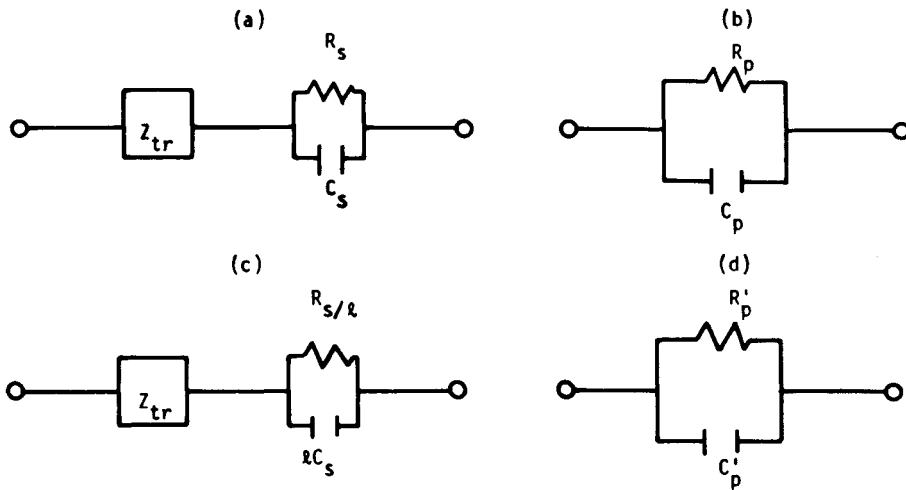Fig. 3. Schematic diagram of low frequency bridge.

Fig. 4. Equivalent circuits for sample and electrode polarization.

Several techniques were used to extract the significant information from the dielectric data collected. Dielectric constant and conductivity values approach constant values at sufficiently high and low frequencies, Fig. 5. In the presence of only one relaxation time τ, the frequency dependence of conductivity and dielectric constant can be expressed by the dispersion equations (Schwan *et al.* (1962)) (5) and (6)

$$\epsilon = \epsilon_\infty + \frac{\epsilon_0 - \epsilon_\infty}{1 + (\omega\tau)^2} \qquad (5)$$

$$\sigma = \sigma_0 + (\sigma_\infty - \sigma_0)\frac{(\omega\tau)^2}{1 + (\omega\tau)^2} \qquad (6)$$

where the terms ϵ_0, ϵ_∞, σ_0 and σ_∞ are limit values of ϵ and σ observed at frequencies which are very small and large, respectively, in comparison to the characteristic frequency f_0. At the characteristic frequency, ϵ and σ are averages, $\epsilon_0 + \epsilon_\infty/2$ and $\sigma_0 + \sigma_\infty/2$ and the dielectric loss $\epsilon'' = (\sigma - \sigma_0/\omega\epsilon_r)$ reaches a peak value.
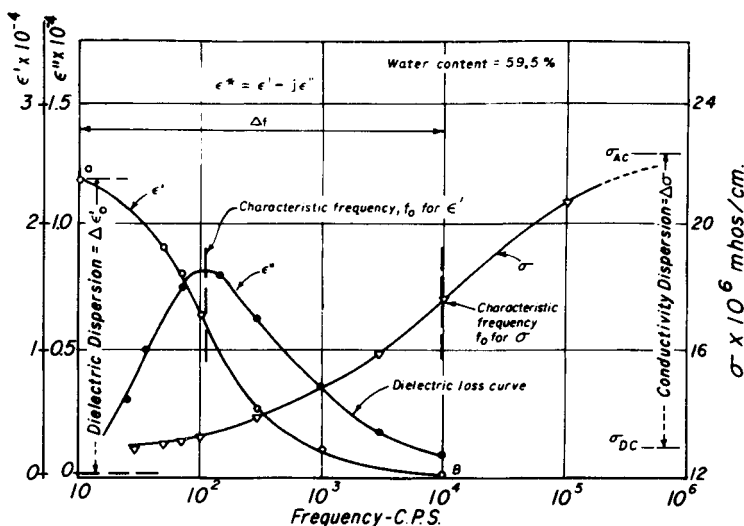
Fig. 5. Conductivity and dielectric dispersion characteristics of saturated
kaolinite hydrite R.

Different values of relaxation times $\tau = 1/2\pi f_0$ are obtained from two curves for ϵ' and σ; the value from the σ curve usually being lower (see Fig. 5). This behavior is in contradiction to Eqs. (5) and (6), which demand that the mean value of ϵ' and σ should occur at the same frequency, f_0. The plot of ϵ'' vs. frequency reaches a peak at a frequency which is virtually equal to the one where ϵ has undergone half its dispersion. It is much lower than the frequency where σ is identical with the mean of σ_0 and σ_∞. This and the fact that the experimental curves are flatter than those calculated from Eqs. (5) and (6) indicate that a spectrum of relaxation times must exist.

Figure 6 shows a typical Cole-Cole plot, i.e. a plot of $(\sigma - \sigma_0/\omega\epsilon_r) = \epsilon''$ vs. ϵ' where ϵ'' is the imaginary part of the complex dielectric constant $\epsilon^* = \epsilon' - j\epsilon''$. This plot yields a circular arc if the distribution function of relaxation times is given by a Cole-Cole distribution function, Cole and

Cole (1941), characterized by an angle α between the radius and the abscissa as indicated in Fig. 6. The data clearly indicate a distribution of relaxation times. The results displayed in Figs. 5 and 6 are typical for all experimental data obtained in this investigation and are indicative of a distribution of relaxation times, τ. The results shown in Fig. 6 correspond to a temperature of 70°F. Similar results obtained on identical samples of sodium kaolinite G-1862, at temperatures of 55°F, 72·5°F, 90°F and 105°F are shown in Fig. 7.

In their simplest form, the relations describing the frequency-response characteristics of complex dielectrics contain four parameters which are necessary and sufficient to define completely the frequency dependencies of both the dielectric constant and the dielectric loss. These parameters are ϵ_0, the dielectric constant measured at low frequency, in a frequency range where ϵ' is independent of frequency; ϵ_∞, the dielectric constant measured at high frequency, also in a range where ϵ' is independent of frequency, τ the "mean relaxation time" for the polarization process giving rise to the "dielectric increment" $(\epsilon_0 - \epsilon_\infty)$, and α the "Cole-Cole parameter", giving a quantitative estimate of the distribution of relaxation times.

Materials tested

The following systems were studied:
(1) Kaolinite (G-1862) with an average equivalent diameter of $0·65\mu$ made homoionic to Na by leaching with 1 N NaCl, followed by leaching with distilled water and finally with 0·01 N NaCl. The leaching with 0·01 N
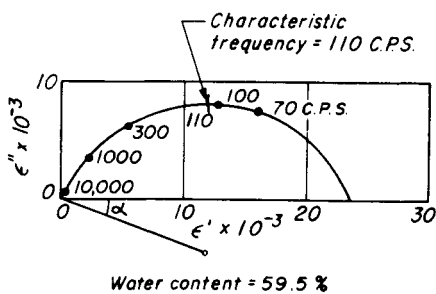

Water content = 59.5 %

Fig. 6. Cole-Cole plot for dielectric dispersion of kaolinite
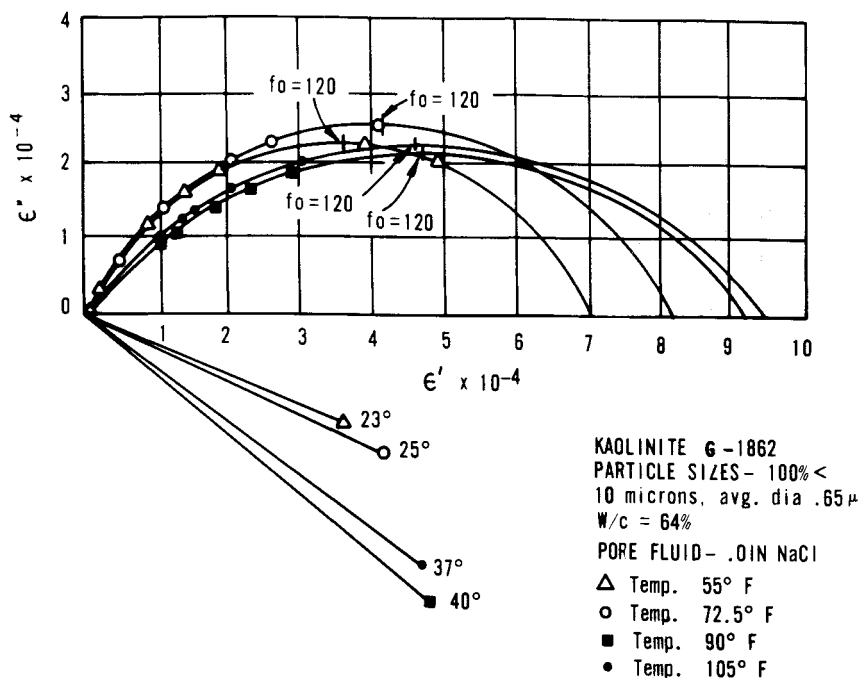hydrite R.

Fig. 7. Cole-Cole plot for dielectric dispersion of Kaolinite G-1862 at different temperatures.

NaCl was carried out until such time as the extract had a conductivity equivalent to 0·01 N NaCl solution. A slurry of the clay was sedimented and consolidated in glass tubes to a water content of 64 per cent. Electrical response characteristics at various temperatures in the range of 55°F–105°F were determined.

(2) Kaolinites ASP 900 and Huber 45 which which have different particle sizes and particle size distributions (Fig. 8) mixed with distilled water to a water content of 75 per cent. The pore fluid conductivity was the same in each case (0.94×10^{-3} mhos/cm).

(3) Hydrite R in media of different and known ionic strengths and samples of Hydrite R in media of different ionic type (K, Na, Li) at 0·01 N concentration. Original samples of Hydrite R were washed with distilled water several times to remove any excess salts, sedimented, and consolidated one dimensionally in glass tubes provided with porous
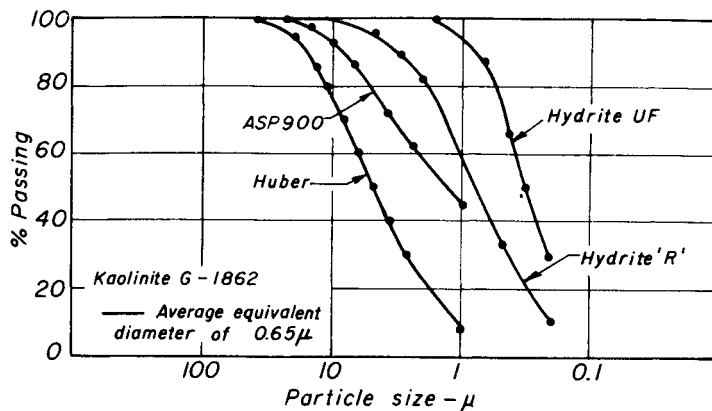
Fig. 8. Particle size distribution of kaolinites.

Table 1. Effects of temperature on electrical properties of saturated kaolinite

Soil type	Temp. °F	Dielectric increment $\Delta\epsilon_0' \times 10^{-4}$	Characteristic frequency f_0, c/s	Low frequency cond. σ_{DC} mhos/cm
	55·0	7·0	120	$0·366 \times 10^{-3}$
Sodium	72·5	8·0	120	$0·480 \times 10^{-3}$
Kaolinite	90·0	9·0	120	$0·600 \times 10^{-3}$
G-1862	105·0	9·5	120	$0·710 \times 10^{-3}$

Dia. of electrode = 1·390″.
Height of sample = 3–5″.
Water content = 64 per cent.
Pore fluid = 0·01 N NaCl.

stones at their bases. At the end of consolidation the samples were leached with 1 N NaCl, 1 N KCl, 1 N LiCl to make samples homoionic to Na, K and Li. Subsequently the samples were leached with distilled water and finally with 0·01 N NaCl, 0·01 N KCl and 0·01 N LiCl until the conductivity of the effluent indicated that the soil water had these concentrations throughout. Similarly samples of Hydrite R were made with soil water concentration of 0·05 N, 0·01 N and 0·002 N NaCl.

(4) Kaolinite Hydrite UF and ASP 900 after consolidation one dimensionally in 6 in. dia. molds. Cylindrical soil specimens of 1·4 in. dia. were cut from the samples with their axes in the direction of consolidation and at right angles to the direction of consolidation.

EXPERIMENTAL RESULTS

The results for clay-water-electrolyte systems are quite similar to those obtained for biological cell suspensions, Schwan (1957). The electrical properties of the kaolinite water-electrolyte system (item 1 above) as a function of temperature are summarized in Table 1. The values in Table 1 were obtained from plots of the type shown in Fig. 5.

It may be seen that the dielectric increment increases with increase in temperature; whereas, the characteristic frequency is independent of temperature. The dielectric increment $(\epsilon_0 - \epsilon_\infty)$ ranges from 7×10^4 to $9·5 \times 10^4$, where ϵ_∞ is of the order of 400.

Table 2 shows the influence of particle size on electrical properties.

These results show that coarser particles yield a higher dielectric increment and a lower characteristic frequency (longer relaxation time) than do the finer particles. The "mean relaxation time" is an inverse measure of the mobility of charge carriers within the dielectric.

The influence of the ionic concentration and ionic type in the suspending medium (item 3 above) on the electrical properties of Kaolinite

Table 2. Effects of particle size and particle size distribution on the electrical properties of saturated kaolinite

Grain size	Soil type	Pore fluid conductivity mhos/cm (Extract)	Dielectric increment $\Delta\epsilon_0' \times 10^{-4}$	Characteristic frequency f_0 c/s
Fine	Kaolinite ASP 900	$0·94 \times 10^{-3}$	21·5	50
Coarse	Kaolinite Huber 45	$0·94 \times 10^{-3}$	53·5	10

Temp. = 69°C–70°F.
Dia. of electrode = 1·390″.
Height of sample = 3–5″.
Pore fluid: Distilled water.
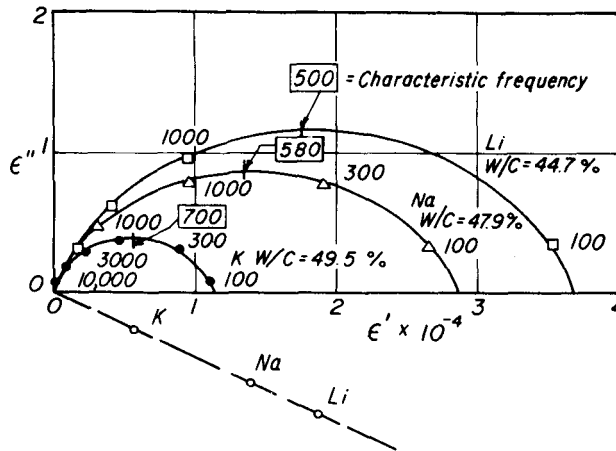Water content: 75 per cent.

Fig. 9. Cole-Cole plot for dielectric dispersion of K, Na, Li Kaolinite.

Hydrite R is significant as may be seen in Table 3. The dielectric behaviour of a Kaolinite (Hydrite R) with different ion types is shown in the form of a Cole-Cole plot in Fig. 9. It can be seen that the larger the hydrated ion size (Li) the larger the dielectric increment and the lower the characteristic frequency, and that the higher the electrolyte concentration the larger the dielectric increment and the characteristic frequency.

It may be noted from these data that the dispersion of the conductivity and dielectric constant and the characteristic frequency are significantly affected by the ion type and ion concentration.

The electrical response characteristics obtained for samples of Hydrite UF and ASP 900 (Kaolinite) where the direction of current is in the direction of consolidation and at right angles to the direction of consolidation are shown in the form of a Cole-Cole plot in Fig. 10. One dimensional consolidation tends to orient the platy clay particles so that their long axes lie in the plane on which the consolidation pressure acts. When particles are aligned with their long axes at right angles to the direction of current, the dielectric increment $(\epsilon_0 - \epsilon_\infty)$ is smaller and the characteristic frequency is larger than when the current is in the direction of orientation of particles. Thus the data show that particle orientation has an influence on the dielectric behavior.

DISCUSSION

Several mechanisms can be examined in terms of their adequacy for explaining the observed behavior.

Debye-Dipolar rotational polarization (1929)

Debye (1929) suggested that the high dielectric constant of water, alcohol and similar liquids resulted from the dipolar nature of their molecules. When an electric field is applied, there is a tendency for the molecules to align themselves with their dipolar axes in the direction of the applied field. Since the dipole polarizations depend upon the relative orientation of molecules, Debye considered that the time required for polarization of this type to form depends upon the internal friction of the material. The time of relaxation
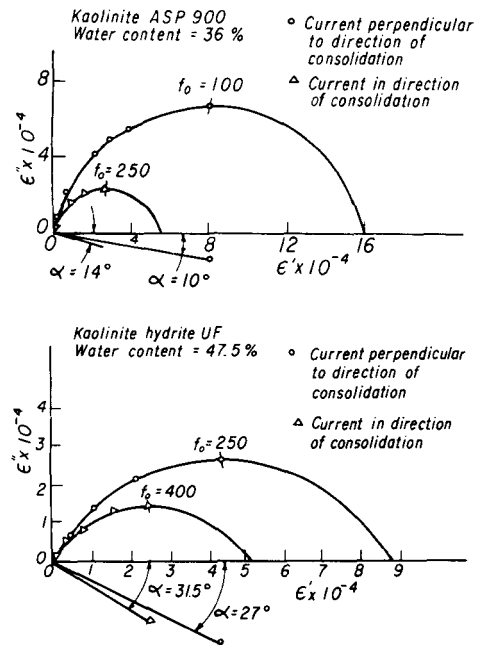

Fig. 10. Effect of orientation of particles on dielectric dispersion.

Table 3a. Effects of electrolyte type and concentration on electrical properties of saturated kaolinite

Soil type	Pore fluid	Hydrated radius of cation (Å)	External electrolyte conc.	Water content (%)	Dielectric increment $\Delta\epsilon_0' \times 10^{-4}$	Characteristic frequency f_0 c/s	Low frequency cond. σ_{DC} mhos/cm	Pore fluid conductivity mhos/cm
					Variable: Electrolyte concentration			
Kaolinite hydrite 'R' consolidated in water, leached with 1N NaCl,	NaCl	5·6–7·9	0·002N	47·3	1·8	450	$0·212 \times 10^{-3}$	$0·25 \times 10^{-3}$
then leached with distilled water, followed	NaCl	5·6–7·9	0·01N	47·9	2·7	580	$0·514 \times 10^{-3}$	$1·53 \times 10^{-3}$
by NaCl of indicated concentration	NaCl	5·6–7·9	0·05N	47·5	2·9	1000	$1·284 \times 10^{-3}$	$4·48 \times 10^{-3}$

Temp. = 69–70°F.
Dia. of electrode = 1·390".
Height of sample = 3–5".

Table 3b. Effect of electrolyte type and concentration on electrical properties of saturated kaolinite

Soil type	Pore fluid	Hydrated radius of cation Å	External electrolyte conc.	Water content (%)	Dielectric increment $\Delta\epsilon_0' \times 10^{-4}$	Characteristic frequency f_0 c/s	Low frequency cond. σ_{DC} mhos/cm	Pore fluid conductivity mhos/cm
					Variable: Type of electrolyte			
Kaolinite hydrite 'R' consolidated in distilled water, leached with	LiCl	7·3–10·3	0·01N	44·7	3·7	500	$0·384 \times 10^{-3}$	$0·83 \times 10^{-3}$
1N, LiCl, NaCl, KCl and then leached with distilled water, followed by	NaCl	5·6– 7·9	0·01N	47·9	2·7	580	$0·574 \times 10$	$1·53 \times 10^{-3}$
0·01N, LiCl, NaCl and KCl as indicated	KCl	3·8–5·32	0·01N	49·5	1·2	700	$0·431 \times 10^{-3}$	$1·01 \times 10^{-3}$

Temp. = 69–70°F.
Dia. of electrode = 1·390″.
Height of sample = 3–5″.

of dipole polarization was expressed in terms of the internal force by the equation

$$t = \frac{\xi}{2KT} = \frac{8\pi\eta a}{2KT} \qquad (7)$$

where ζ is the internal friction coefficient, η is the coefficient of viscosity, a is the radius of the

$$\tau = \frac{\epsilon_i + 2\epsilon_a - p(\epsilon_i - \epsilon_a)}{\sigma_i + 2\sigma_a - p(\sigma_i - \sigma_a)} \qquad (8)$$

$$\sigma_0 = \frac{\sigma_a(\sigma_i + 2\sigma_a) + 2p(\sigma_i - \sigma_a)}{(\sigma_i + 2\sigma_a) - p(\sigma_i - \sigma_a)} \qquad (9)$$

$$\epsilon_\infty = \epsilon_a \frac{(\epsilon_i + 2\epsilon_a) + 2p(\sigma_i - \sigma_a)}{(\epsilon_i + 2\epsilon_a) - p(\epsilon_i - \epsilon_a)} \qquad (10)$$

$$\sigma_1 = \sigma_0 + 9p(1-p) \frac{(\epsilon_a\sigma_i - \sigma_a\epsilon_i)^2}{[(\epsilon_i + 2\epsilon_a) - p(\epsilon_i - \epsilon_a)]^2[(\sigma_i + 2\sigma_a) - p(\sigma_i - \sigma_a)]} \qquad (11)$$

$$\epsilon_0 = \epsilon_\infty + 9p(1-p) \frac{(\epsilon_a\sigma_i - \sigma_a\epsilon_i)^2}{[(\epsilon_i + 2\epsilon_a) - p(\epsilon_i - \epsilon_a)][(\sigma_i + 2\sigma_a) - p(\sigma_i - \sigma_a)]^2} \qquad (12)$$

molecule, T is the absolute temperature and K is Boltzmann's constant. This expression for τ is based on Stoke's Law for a free body.

Thus according to Debye's theory an increase in temperature should cause a decrease in dielectric constant. This decrease in ϵ' results from the increased thermal energy which makes it more difficult to align dipoles in the direction of the field.

The results shown in Table 1 indicate, however, that ϵ_0 increases with increase in temperature and the relaxation time τ is constant with an increase in temperature. Thus the results cannot be explained by the Debye-dipolar rotational mechanism.

Maxwell-Wagner, Pauley and Schwan interfacial polarization

Maxwell (1873), employing the simplest possible model of an inhomogeneous dielectric consisting of plane sheets of materials having different ratios of conductivity to dielectric constant, was able to provide a plausible qualitative explanation of the sort of phenomena observed in some actual dielectrics. Wagner (1914) extended Maxwell's theory by assuming that the conducting particles were spheres, sparsely distributed throughout a material of comparatively low dielectric loss.

When a current is passed through such a system, accumulation of charges is considered to occur at interfaces. For accumulation of charges to occur at the interface, the charges must flow through a layer of dielectric whose resistance may be high enough that the interface does not become completely charged during the time allowed for charging. For the alternating current case, this implies a decrease of capacity, hence a decrease of dielectric constant with increasing frequency.

Pauley and Schwan (1959) extended Wagner's equations, which apply for low volume concentration of particles, to higher volume concentrations and showed that

where ϵ_r is the dielectric constant of vacuum $(8.85 \times 10^{-4}\ F/cm)$ ϵ_i and ϵ_a are the dielectric constants of particle and solution relative to vacuum, p is the volume fraction of the particles and σ_i and σ_a are the conductivity of the particle and the solution respectively.

According to this theory, the relaxation process can be shown to occur in the frequency range of 10^6–10^9 c/s. If it is assumed that the dielectric constant for dry clay particles $\epsilon_i = 2.5$, $\sigma_i = 0$, $\epsilon_a = 78$ for water-electrolyte solution, $\sigma_a = 0.1 \times 10^{-3}$–$10 \times 10^{-3}$ mhos/cm. (conductivity of 0.001 N–0.1 N NaCl solution), $p = 0.3$, and $\sigma_i = 0$, and these values are substituted in Eq. (8) for relaxation time, the characteristic frequency $(f_0 = 1/2\pi\tau)$ lies between 2 and 200 mc. The change of dielectric constant $(\epsilon_0 - \epsilon_\infty)$ obtained from Eq. (12), when the above values are substituted is about 0.1. Further, Eq. (8) shows that relaxation time is independent of particle size, and, hence, one relaxation time is predicted even in the case of different particle sizes. Equation (12) shows that the dispersion characteristics are dependent on properties of the various components, such as dielectric constant and conductivity, but independent of particle size.

Results shown in Fig. 5 and in Tables 1–3 indicate that the value of $(\epsilon_0 - \epsilon_\infty)$ is above 10^4, and the characteristic frequency is in the kilocycle range. Results summarized in Table 2 show that the relaxation time and dielectric increment are dependent on particle size and particle size distribution. The Maxwell-Wagner, Pauley and Schwan type of polarization therefore do not appear to account for the observed data.

O'konski's theory of ionic polarization

O'konski (1960) treated the dielectric behaviour of colloidal particles by introducing the concept of surface conductivity. He assumed that the surface conductivity, λ, is composed of two parts; λ_s, the

contribution of all charge carriers in the surface, λ_a, the contribution to the conductivity due to the ion atmosphere. Thus

$$\lambda = \lambda_s + \lambda_a \qquad (13)$$

where the quantity λ_s is given by

$$\lambda_s = \Sigma \, S_i U_i Z_i \qquad (14)$$

and U_i is the mobility of a carrier of type i.

S_i is the number of carriers per unit surface area
Z_i is the valence

In an alternating current field it is considered that the density of free charges at the surface undergoes a time variation as a result of two processes:
(a) The transport of ions to and from an element of surface as a result of different bulk conductivities of the two media, spherical particles and solvent.
(b) The transport of ions along the surface as a result of surface conductivity.
According to O'konski, the dielectric increment is dependent upon the conductivity ratio, r, which involves both the conductivity of the solvent σ_a and the surface conductivity, $2\lambda/R$, where R is the radius of the particle. The conductivity ratio $r = 2\lambda/R\sigma_a$ where σ_i the conductivity of the clay particle is taken as zero.

If it is assumed that the conductivity of the solvent $\sigma_a = 0.001$ mhos/cm, the surface conductance, λ, is of the order of 10^{-6} mhos, and the radius of the particle is 2μ, then the value of $2\lambda/R$ would be 0.01, and the value of r would be 10. The dielectric increment, $\Delta\epsilon$, (in a dilute suspension) at low frequencies, $\omega \to 0$, according to O'konski (1960) would be

$$\left(\frac{\Delta\epsilon}{p}\right)_{\substack{\omega\to 0 \\ p\to 0}} = \frac{3[(r^2 - 2r - 2)\epsilon_a + 3\epsilon_i]}{(r+2)^2} \qquad (15)$$

for $\epsilon_a = 75$, $\epsilon_i = 3$

$$\left(\frac{\Delta\epsilon}{p}\right)_{\substack{\omega\to 0 \\ p\to 0}} = 122$$

The values of $\Delta\epsilon$ observed are in the order of 10^4–10^5 for particle volume concentration of 0.4, hence O'konski's theory would not appear able to explain the data. It is pertinent to note, however, that Eq. (15) was developed for dilute suspensions.

Schwarz's theory of double layer polarization

Schwarz (1962) has shown that, if a nonconductive spherical particle surrounded by an electric double layer is suspended in a conducting medium,

an electric field applied to the medium will cause counterion migration in the plane of the double layer. The extent of the counterion polarization within the double layer will depend upon the counterion mobility and surface concentration, and is opposed by the tendency of the ions to counterdiffuse and eliminate the surface concentration gradient. This double-layer polarization leads to an increase in the dielectric constant, which can be substantially greater than that contributed by the bulk phases. The pertinent equations relating the dielectric increment and the relaxation time (assuming no distribution of times) to radius of particle, R; volume concentration of particles, p; counterion density in the double layer, X_0 (cm^{-2}); the electronic charge, e_0; the absolute dielectric constant of vacuum, ϵ_r; the ion mobility, u (cm.sec.$^{-1}$dyne^{-1}); the Boltzmann constant, K; and the absolute temperature, T; are

$$\Delta\epsilon_0 = \epsilon_0 - \epsilon_\infty = 9/4 \frac{p}{(1+p/2)^2} \frac{e_0^2 R X_0}{\epsilon_r K T} \qquad (16)$$

$$\tau = \frac{R^2}{2UKT} \qquad (17)$$

Equation (16) shows that the dielectric increment (per particle) is greater the higher the double layer charge density and the larger the radius of the sphere. Furthermore, the relaxation time for the polarization is proportional to the square of the sphere radius and inversely proportional to the diffusion coefficient $(D = UKT)$. According to Eq. (17) a variation of ionic mobilities within the double layer and a spread of particle sizes, can lead to a relaxation-time distribution. If appropriate values of particle radius, particle volume concentration, surface charge density and ionic mobilities are substituted in Eq. (16) and (17) the theory predicts $(\epsilon_0 - \epsilon_\infty) \simeq 10^4$–$10^5$ and dispersion occurs in the low frequency kilocycle range. As an example, for a kaolinite-water-electrolyte system (G-1862, Table 1) an average radius of the particle has been found to be $0.32\,\mu$ (page 341). Assuming a cation exchange capacity of 5 meq/100 g, and a specific surface area of 15×10^4 cm^2/g, the surface charge density, X_0, can be shown to be equal to

$$X_0 = \frac{6.02 \times 10^{20} \times 0.05}{15 \times 10^4}$$

$$= 2 \times 10^{14} \text{ charges/cm}^2 = 2 \times 10^{18} \text{ charges/m}^2$$

For a water content of 64 per cent and a specific gravity of particles of 2.6, the void ratio, $e = 2.6 \times 0.64 = 1.66$ and the particle volume concentration $p = 1/1 + e = 0.38$. Hence $p/(1+p/2)^2 = 0.273$.

$$\frac{9/4e_0{}^2}{\epsilon_r KT} = \left(\frac{9}{4}\right) \frac{(1 \cdot 6 \times 10^{-19})^2}{8 \cdot 85 \times 10^{-12} \times 1 \cdot 38 \times 10^{-23} \times 291}$$

$$= 1 \cdot 63 \times 10^{-6}$$

Substituting these values in Eq. (16) gives

$$\Delta \epsilon_0 = 0 \cdot 273 \times 1 \cdot 63 \times 10^{-6} \times 0 \cdot 32 \times 10^{-6} \times 2 \times 10^{18}$$

$$= 28 \cdot 4 \times 10^4$$

The measured values of $\Delta \epsilon_0$ are of the same order of magnitude as those expected according to Schwarz's theory.

According to Schwarz's model the characteristic frequency

$$f_0 = \frac{1}{2\pi\tau} = \frac{2D}{2\pi R^2} = \frac{D}{\pi R^2}$$

(From Eq. (17), $\tau = R^2/2D$, where $UKT = D$, the diffusion coefficient). Substituting a value of $D \simeq 10^{-5}$ cm²/sec and $R = 1\ \mu$ gives a value for

$$f_0 = \frac{10^{-5}}{\pi \times 10^{-8}} = \frac{1000}{\pi} \simeq 200 \text{ c/s.}$$

This value of $f_0 = 300$ c/s is in the range of frequencies observed experimentally.

Schwarz's model, therefore, leads to prediction of essentially the same kind of dielectric behaviour as is observed in this investigation.

This theory, however, like most of the other theories does not consider effects on the electrical properties caused by particle orientation and the degree of binding of the ion to the surface. That electrical properties are influenced by the orientation of particles is clear from the results shown in Fig. 10. Further the results shown in Fig. 9 show the influence of binding of ions to the surface. The strength of the electrostatic attraction of the positive counter-ions to the negatively charged surface depends on the ionic charge and the distance of closest approach between the counterion and the fixed charges in the surface. The distance of closest approach a^0, called Debye–Huckel parameter, for univalent ions follows the sequence (Hellfferich 1962)

$$K^+ < Na^+ < Li^+$$

Hence a K^+ ion is strongly attracted to the surface and its binding tendency to the surface is larger than that of Li^+ ion. Thus the smaller value of $(\epsilon_0 - \epsilon_\infty)$ in K clay (see Fig. 9) as compared to the Na or Li clay may be due to the difference in binding tendency of the ions.

Further Schwarz's theory does not consider the influence of electrolyte concentration on dielectric behavior. The amount of electrolyte has a significant influence on the dielectric behavior as seen from results summarized in Table 3. The larger electrolyte concentration producing larger dielectric increment and larger characteristic frequency (f_0) or smaller relaxation time ($\tau = 1/2\pi f_0$) $D(\tau = R^2/2UKT = R^2/2D)$. In spite of these limitations, the basic idea that the double layer polarization controls the relaxation effects appear reasonable, and possibly the theory of Schwarz may be modified to take into account the above factors.

CONCLUSION

The results of this investigation have revealed that clay-water electrolyte systems behave as anamolous dielectrics as found by others (see Gillespie (1956), Goldsmith (1960), Smity-Rose (1923)) in the audio frequency and near radio frequency range. Like biological cells they display astronomically large dielectric constants and dielectric loss at low frequencies and exhibit very broad dielectric dispersion. The dielectric constant increases with increase in particle size, ion size, temperature and electrolyte concentration. The characteristic frequency decreases with increase in particle size, decrease in ion size, increase in electrolyte concentration and remains constant with increase in temperature. Particle orientation has a significant influence on the magnitude of dielectric dispersion and relaxation time. Larger dielectric increment and lower relaxation time is observed when the current is parallel to the long axis of the particles as compared to when the current is perpendicular to the long axis of the particles. The distribution of relaxation time observed in almost all cases can be quantitatively characterized by the Cole-Cole parameter α. The dispersion spectrum is determined by the particle size distribution and the ion mobility. This above behavior has been judged to be due to the displacement of the charges within the electric double layer and the theory of Schwarz in part can be used to explain the data.

It is considered that the characterization of soils may be attempted in terms of the electrical parameters $\epsilon_0 - \epsilon_\infty$, the dielectric increment, f_0, the characteristic frequency and α, the Cole-Cole distribution parameter.

нтация, тип и количество электролита, а также температура влияют на низкочастотное диэлектрическое приращение и на среднее время релаксации. Ряд физических процессов, как например релаксация, вызванная биполярной вращателъной поляризацией, межповерхностная поляризация, пространственный заряд и поляризация связанных ионов, исследуются с целъю объяснения наблюдаемых данных. Вывод доклада, что в данное время нет теории для объяснения всех данных, но механизм поляризации связанных ионов повидимому объясняет некоторые резулътаты.